The Astrophysical Journal, 604:L93–L96, 2004 April 1

BULGES OR BARS FROM SECULAR EVOLUTION?

Victor P. Debattista and C. Marcella Carollo
Institut für Astronomie, ETH Hönggerberg, CH-8093 Zürich, Switzerland; debattis@phys.ethz.ch, marcella.carollo@phys.ethz.ch
and
Lucio Mayer and Ben Moore
Department of Theoretical Physics, University of Zürich, Winterurestrasse 190, 8057 Zürich, Switzerland; lucio@physik.unizh.ch, moore@physik.unizh.ch
Received 2003 November 11; accepted 2004 February 19; published 2004 March 3

ABSTRACT

We use high-resolution collisionless *N*-body simulations to study the secular evolution of disk galaxies and, in particular, the final properties of disks that suffer a bar and perhaps a bar-buckling instability. Although we find that bars are not destroyed by the buckling instability, when we decompose the radial density profiles of the secularly evolved disks into inner Sérsic and outer exponential components, for favorable viewing angles, the resulting structural parameters, scaling relations, and global kinematics of the bar components are in good agreement with those obtained for bulges of late-type galaxies. Round bulges may require a different formation channel or dissipational processes.

Subject headings: galaxies: bulges — galaxies: evolution — galaxies: formation — galaxies: kinematics and dynamics — galaxies: photometry — galaxies: spiral

1. INTRODUCTION

Evidence has accumulated in the past decade showing that many bulges, especially at low masses, have a disklike, almost exponential radial falloff of the stellar density (Andredakis & Sanders 1994; Courteau, de Jong & Broeils 1996; de Jong 1996; Carollo, Stiavelli, & Mack 1998; Carollo et al. 2001; Carollo 1999; MacArthur, Courteau, & Holtzman 2003) and, in some cases, disklike, cold kinematics (Kormendy 1993; Kormendy, Bender, & Bower 2002). Comparisons of bulge and disk parameters have furthermore shown a correlation between the scale lengths of bulges and disks (de Jong 1996; MacArthur et al. 2003) and, on average, similar colors in bulges and inner disks (Terndrup et al. 1994; Peletier & Balcells 1996; Courteau et al. 1996). The disklike properties of bulges and the links between bulge and disk properties have been suggested to indicate that bulges may form through the evolution of disk dynamical instabilities such as bars, which are present in about 70% of nearby disk galaxies (Knapen 1999; Eskridge et al. 2000).

It has long been known that bars lead to angular momentum redistribution and to an associated increase in the central mass density. Already Hohl (1971) found that an initially single component disk evolved a double exponential density profile under the influence of a bar; as a result, the scale length of the outer disk increases. It has been suggested that bars may be efficient at building *three-dimensional* stellar bulgelike structures via scattering of stars at vertical resonances (Combes et al. 1990), or by the collisionless buckling instability (which weakens the bar; Raha et al. 1991), or via bar destruction due to the growth of a central mass concentration (Pfenniger & Norman 1990; Norman, Sellwood, & Hasan 1996). As buckling occurs relatively easily, it could be a particularly promising avenue for bulge formation. This instability leads to the large-scale, coherent bending of the bar perpendicular to the plane of the disk (Raha et al. 1991). Buckling, which is a result of vertical anisotropy (Araki 1985; Fridman & Polyachenko 1984; Merritt & Hernquist 1991; Merritt & Sellwood 1994), thickens the stellar system and weakens the bar. Evidence that buckling occurs in nature has relied on the fact that buckled bars are boxy/peanut-shaped when viewed edge-on and on the unmistakable gas-kinematic signature of a bar observed in such bulges (Kuijken & Merrifield 1995; Merrifield & Kuijken 1999; Bureau & Freeman 1999). The relevance of buckling to bulge formation remains rather anecdotal, however, as little work has been done to check that the structural and kinematic properties of buckled bars are quantitatively consistent with those observed in bulges.

In this Letter, we report on high-resolution *N*-body simulations of bar-unstable disks, some of which buckle, and compare their secularly evolved structural and kinematic properties with those of bulges in local galaxies. We describe our simulations in § 2, present our results in § 3, and discuss their implications in § 4.

2. METHODS

2.1. *Rigid-Halo Simulations*

Most of the *N*-body simulations reported in this Letter consist of a live disk inside a rigid halo, which allows large numbers of particles and high spatial resolution. The rigid halos were represented by either a logarithmic potential, $\Phi_L = v_h^2/2 \ln (r^2 + r_h^2)$, or a Hernquist potential, $\Phi_{\rm H} = -M_h/(r + r_h)$. The initially axisymmetric disks were modeled by the generalized surface density profile $I(r) \propto \exp [-(r/r_0)^{(1/n)}]$ introduced by Sérsic (1968). This gives a de Vaucouleurs (1948) profile for $n = 4$ and an exponential profile for $n = 1$; we used $1 \leq n \leq 2.5$. The disks have scale length R_d, mass M_d, Gaussian thickness z_d, and are truncated at a radius R_t. Disk kinematics were set up using the epicyclic approximation to give a constant Toomre Q-parameter, which we varied from 1.2 to 2.0. Vertical equilibrium was obtained by integrating the vertical Jeans equation. The disks were represented by $(4–7.5) \times 10^6$ equal-mass particles. We use units where $R_d = M = G = 1$; thus, the unit of time is $(R_d^3/GM)^{1/2}$.

The simulations were run using a three-dimensional cylindrical polar grid code (Sellwood & Valluri 1997) with $N_R \times N_\phi \times N_z = 60 \times 64 \times 243$. The radial spacing of grid cells increases logarithmically from the center, reaching to $\sim 2R_t$; in all cases, $R_t = 5$. The vertical spacing, δz, of the grid planes was set such that $0.2 \geq z_d \geq 0.025 \geq 4\delta z$. We used Fourier terms up to $m = 8$ in the potential, with a Plummer softening

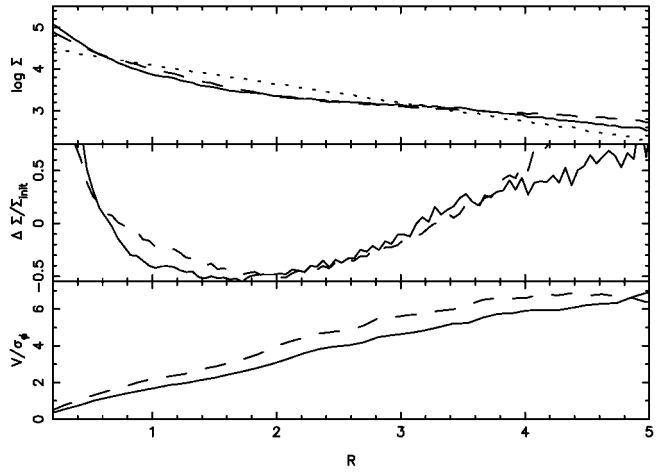

FIG. 1.—Comparison of the evolution of the density profiles in matched live- (*solid lines*) and rigid-halo (*dashed lines*) simulations after ~2.4 Gyr. In the top panel, the initial profile is indicated by the dotted line. The fractional change in the profiles, relative to the initial profile, is shown in the middle panel. The bottom panel shows the profile of V/σ_ϕ.

length $\epsilon = 0.017$. We verified that our results are not sensitive to resolution by running the most strongly buckled model with $m = 32$ and smaller δz. Time integration was performed with a leapfrog integrator with a fixed time step, $\delta t = 0.01$ for all runs except for the $n > 1$ simulations, for which we used $\delta t = 0.0025$. We chose values for the halo parameters such that our rotation curves were approximately flat to large radii. For the logarithmic halos, we set $v_h = 0.68$, while the Hernquist halos had $M_h = 43.4$. We measured the amplitudes of the bar, A_ϕ, and of buckling, A_z, as the normalized amplitudes of the $m = 2$ tangential and vertical density distributions. We will discuss the effects of different initial conditions elsewhere.

2.2. *Modeling and Measured Parameters*

In order to compare our final systems with observed galaxies, we first obtained, for all simulations, radial density profiles of the disk mass density distribution at three inclinations: $i = 0$ (face-on), $i = 30°$, and 60°. For $i = 0$, we simply computed the azimuthally averaged mass profile. For $i = 30°$ and 60°, we considered three orientations of the bar with respect to the major axis ($\phi_{\rm bar} = 0$, 45°, and 90°); we then measured the one-dimensional projected surface density profiles with the task ELLIPSE in IRAF.[1]

We decomposed these mass profiles into a central Sérsic component plus an outer exponential disk; a Sérsic law is usually used in modeling bulge light profiles (Andredakis, Peletier, & Balcells 1995; Graham 2001; MacArthur et al. 2003). We stress that by decomposing the final density profiles into a "bulge" plus disk component, we are not implying that secular evolution has produced three-dimensional bulges. Nonetheless, for brevity, we will refer to as "bulges" the central Sérsic components and as "disks" the exponential components.

Our Sérsic bulge plus exponential disk decompositions are characterized by five parameters: $\Sigma_{0,d}$ and $\Sigma_{0,b}$, the disk and the bulge central surface densities, respectively; R_d, the scale length of the outer exponential disk; $R_{b,\rm eff}$, the half-light radius of the bulge; and n_b, the index of the Sérsic profile. In light of the ill-conditioned fitting described by MacArthur et al. (2003), n_b was held fixed with respect to the remaining four parameters when searching for the best-fitting models; the best-fitting n_b was then identified as the one giving the smallest χ^2 when repeating the fits with $0.1 \le n_b \le 4$ in steps of 0.1. The five parameters derived from the bulge/disk decompositions allow us to compute three dimensionless structural quantities to compare with observations: n_b, $R_{b,\rm eff}/R_d$, and B/D, the ratio of bulge to disk mass (we assumed a constant mass-to-light ratio when comparing with the light-weighted measurements available for real galaxies).

We also measured the bulge ellipticity, ϵ_b, the line-of-sight velocity dispersion, $\bar{\sigma}$ (by averaging the corresponding profiles within some radial range), and the peak line-of-sight velocity within the same radial range on the disk major axis, V_p. These allow us to compute $V_p/\bar{\sigma}$ to investigate the kinematic properties of the resulting bulges in the $V_p/\bar{\sigma}$ versus ϵ_b plane. In this plane, normal bulges are thought to follow the locus traced by isotropic oblate rotators (Binney & Tremaine 1987), and bulges that result from the secular evolution of disks are thought to emerge as systems that are dynamically colder than isotropic oblate rotators (Kormendy 1993; Kormendy et al. 2002).

2.3. *Live-Halo Simulation*

Rigid-halo simulations are better suited to systems in which the disk is dominant in the inner regions (as are the simulations discussed here), because the interaction with the halo is then weaker. While massive disks represent a reasonable assumption for high surface brightness barred galaxies (Debattista & Sellwood 2000), it is important to verify that the full interaction with a live dark matter (DM) halo does not lead to a drastically different evolution for the structural and kinematic parameters. The ability of a bar to lose angular momentum to a DM halo helps make it stronger (Debattista & Sellwood 2000). We therefore have run a pair of matched live- and rigid-halo simulations. The live-halo simulations were run on PKDGRAV (Stadel 2001; details of the live-halo simulations will be presented elsewhere). We checked that these results are not sensitive to resolution by running the live-halo model with larger N and smaller ϵ. The two simulations evolved differently: the bar in the live-halo case was slightly stronger and slows down because of dynamical friction with the halo. Nonetheless, the mass density and V/σ_ϕ profiles in the rigid- and live-halo simulations remain quite similar, as we illustrate in Figure 1 (we use σ_ϕ in this comparison because it is representative of what we might expect in high-inclination observations). The larger central density in the live-halo simulation of Figure 1 is a result of the fact that its bar can shed additional angular momentum. Otherwise, this comparison suggests that the gross features seen in the live-halo simulation are well reproduced by the rigid-halo simulation, giving confidence that the rigid-halo simulation survey from which we draw the main conclusions of this Letter is adequate to describe the evolution of massive disks. Moreover, by using rigid halos, we assure that we obtain a minimal level of bar secular evolution, which helps to disentangle the effects of different evolutionary processes.

3. RESULTS

3.1. *Time Evolution*

The evolution of a representative strongly buckling simulation, shown in Figure 2, produced a bar by $t \simeq 50$, which then buckled strongly at $t \simeq 100$. Despite the strong buckling, the bar is weakened but not destroyed. As is well known, the process of bar

[1] IRAF is distributed by NOAO, which is operated by AURA, Inc., under contract with the National Science Foundation.

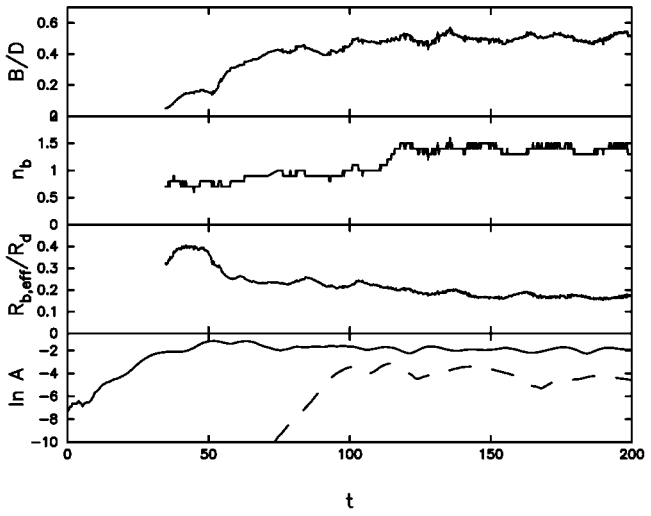

FIG. 2.—Evolution of a representative strongly buckling simulation. From bottom to top, the panels show the evolution of A_ϕ (strength of bar; *solid line*) and A_z (strength of buckling; *dashed line*), $R_{b,\,\mathrm{eff}}/R_d$, n_b, and B/D, all measured at $i = 0$. The bar forms at $t \simeq 50$ and buckles at $t \simeq 100$. Before $t = 30$, the fitting algorithm is unstable, and spurious results are obtained because the algorithm fits the transient spiral structure.

formation drives a redistribution of angular momentum, leading to an increase in the central density. This process is largely complete by the time the bar buckles: the buckling instability does not alter significantly the scale length or the mass of the inner Sérsic component. However, it is interesting that at buckling, n_b changes from $n_b \simeq 1$ to $n_b \simeq 1.5$; thus, buckling may contribute to the scatter of n_b around the exponential value observed in the bulges of real intermediate-type galaxies.

3.2. *Comparisons with Observations*

In Figure 3, we compare the structural properties of our final systems with similar quantities measured for local bulges. Our simulations are represented by filled symbols when ϵ_b is larger than the ellipticity of the disk, $\epsilon_d \equiv 1 - \cos i$. All $i \leq 30°$ projections have $\epsilon_b > \epsilon_d$, as are about half of the projections at $i = 60°$. Bulges in our simulations cover a broad range of parameter space, including regions where no real bulges are found. This mismatch is diminished when only systems with $\epsilon_b < \epsilon_d$ are considered, but at the cost that a large fraction of the projections, including all at $i \leq 30°$, are excluded from the sample. Nevertheless, the overlap between the simulations and the observations is quite good.

We also checked whether global kinematics can distinguish between bona fide bulges and bulgelike bars. In Figure 4, we plot $V_p/\bar{\sigma}$ versus ϵ_b for real bulges and for our simulations. For real bulges, V_p and $\bar{\sigma}$ were obtained by fitting a de Vaucouleurs profile to the bulge. Our simulations are rather poorly fitted by a de Vaucouleurs profile, which introduces a systematic difference between our measurements and Kormendy's (1993). To quantify some of this uncertainty, we have measured ϵ_b, V_p, and $\bar{\sigma}$ within $R_{b,\,\mathrm{eff}}$ and $R_{b,\,\mathrm{eff}}/2$ and used half the difference as our error estimate. This diagram shows that evolved bars can show, under some viewing angles, global kinematic-elongation properties typical not only of the dynamically cold "pseudobulges" but also those that are taken as *defining* the bona fide, dynamically hot bulges. These are the expected projection effects for triaxial spheroids seen at high inclination (e.g., Binney & Tremaine 1987). Thus, the population of bulges that are identified

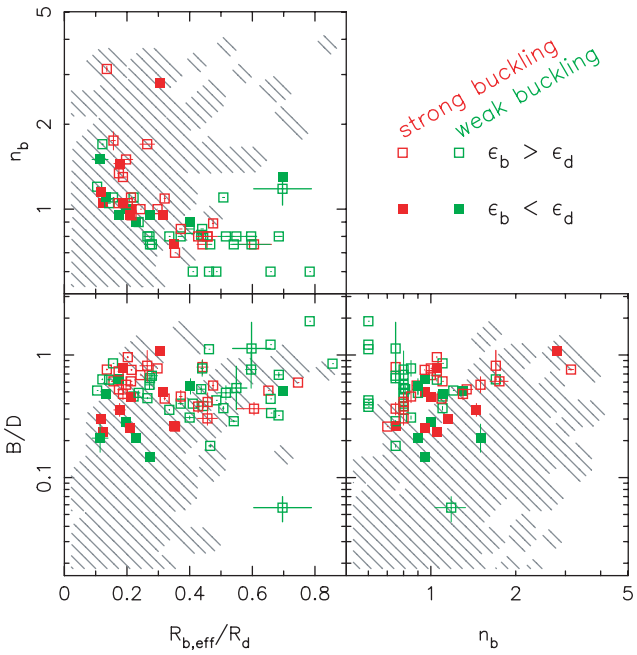

FIG. 3.—Structural properties of our simulations compared with observed galaxies (*shaded area*) from MacArthur et al. (2003) and Graham (2003). Squares are filled (empty) when $\epsilon_b < \epsilon_d$ ($\epsilon_b > \epsilon_d$) and are red (green) when buckling is strong (weak).

by bulge/disk decompositions or by kinematics may have some contribution from bars.

4. DISCUSSION

Although Raha et al. (1991) only reported bar weakening, not destruction, by the buckling instability, it has become common wisdom that buckling destroys bars. Our simulations have failed to turn up a single instance in which the bar was destroyed by buckling, although we cannot exclude that it is in some extreme case. The channel of bulge formation by the dissipationless destruction of bars during buckling, therefore, is not viable.

However, the minimal collisionless secular evolution present in our simulations must also occur in nature, resulting in sys-

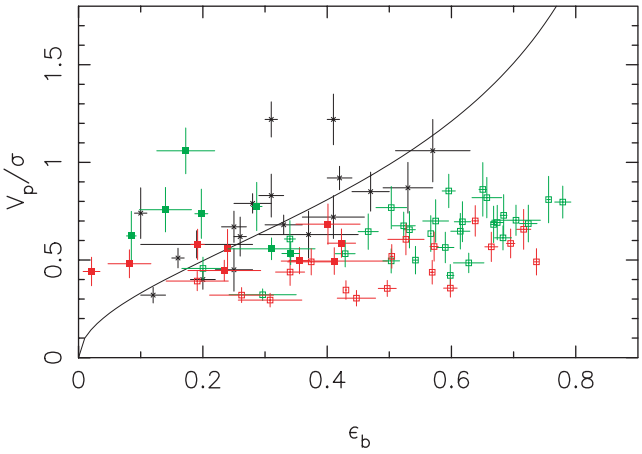

FIG. 4.—$V_p/\bar{\sigma}$ vs. ϵ_b diagnostic plane. Symbols for simulations are as in Fig. 3, while the observational data of Kormendy (1993) are indicated by the black asterisks.

tems that exhibit double-component mass density profiles. For certain viewing orientations, the spread in structural parameters and kinematic properties is indistinguishable from those observed in systems that are classified as bulges.

Nonetheless, the existence in nature of round bulges inside low-inclination galaxies, which our simulations cannot reproduce, requires that other processes are also involved. Possibly secular evolution including dissipative gas (Mayer & Wadsley 2004) will result in rounder bulges, but this requires extended central objects with masses of ~10%–20% that of the disk (Shen & Sellwood 2004). The higher interaction rate in the early universe may have triggered the large gas inflows needed to build such objects.

Finally, because the halos of our simulations are rigid, the baryonic component cannot but conserve its angular momentum. In (semi-) analytic models of disk galaxy formation (Fall & Efstathiou 1980; Mo, Mao, & White 1998; Lacey & Silk 1991; White & Frenk 1991; Dalcanton, Spergel, & Summers 1997; van den Bosch 1998), the distribution of disk scale lengths, R_d, is set by that of their angular momenta. De Jong & Lacey (2000) found that the width of the observed R_d distribution at fixed luminosity is smaller than that predicted by analytic theory. Our simulations show that, under the influence of a bar, R_d may increase by a factor of 2 or more at constant global angular momentum. Since less extended disks are likely to be more bar-unstable, the secular evolution of these disks may be responsible for at least part of this discrepancy.

We would like to thank the anonymous referee for useful suggestions.

REFERENCES

Andredakis, Y. C., Peletier, R. F., & Balcells, M. 1995, MNRAS, 275, 874
Andredakis, Y. C., & Sanders, R. H. 1994, MNRAS, 267, 283
Araki, S. 1985, Ph.D. thesis, MIT
Binney, J., & Tremaine, S. 1987, Galactic Dynamics (Princeton: Princeton Univ. Press)
Bureau, M., & Freeman, K. C. 1999, AJ, 118, 126
Carollo, C. M. 1999, ApJ, 523, 566
Carollo, C. M., Stiavelli, M., de Zeeuw, P. T., Seigar, M., & Dejonghe, H. 2001, ApJ, 546, 216
Carollo, C. M., Stiavelli, M., & Mack, J. 1998, AJ, 116, 68
Combes, F., Debbasch, F., Friedli, D., & Pfenniger, D. 1990, A&A, 233, 82
Courteau, S., de Jong, R. S., & Broeils, A. H. 1996, ApJ, 457, L73
Dalcanton, J. J., Spergel, D. N., & Summers, F. J. 1997, ApJ, 482, 659
Debattista, V. P., & Sellwood, J. A. 2000, ApJ, 543, 704
de Jong, R. S. 1996, A&A, 313, 45
de Jong, R. S., & Lacey, C. 2000, ApJ, 545, 781
de Vaucouleurs, G. 1948, Ann. d'Astrophys., 11, 247
Eskridge, P. B., et al. 2000, AJ, 119, 536
Fall, S. M., & Efstathiou, G. 1980, MNRAS, 193, 189
Fridman, A. M., & Polyachenko, V. L. 1984, Physics of Gravitating Systems (New York: Springer)
Graham, A. W. 2001, AJ, 121, 820
———. 2003, AJ, 125, 3398
Hohl, F. 1971, ApJ, 168, 343
Knapen, J. H. 1999, in ASP Conf. Ser. 187, The Evolution of Galaxies on Cosmological Timescales, ed. J. E. Beckman & T. J. Mahoney (San Francisco: ASP), 72
Kormendy, J. 1993, in Galactic Bulges, ed. H. Dejonghe & H. J. Habing (Dordrecht: Kluwer), 209
Kormendy, J., Bender, R., & Bower, G. 2002, in ASP Conf. Ser, 273, The Dynamics, Structure and History of Galaxies, ed. G. S. Da Costa & H. Jerjen (San Francisco: ASP), 29
Kuijken, K., & Merrifield, M. R. 1995, ApJ, 443, L13
Lacey, C., & Silk, J. 1991, ApJ, 381, 14
MacArthur, L. A., Courteau, S., & Holtzman, J. A. 2003, ApJ, 582, 689
Mayer, L., & Wadsley, J. 2004, MNRAS, 347, 277
Merrifield, M. R., & Kuijken, K. 1999, A&A, 345, L47
Merritt, D., & Hernquist, L. 1991, ApJ, 376, 439
Merritt, D., & Sellwood, J. A. 1994, ApJ, 425, 551
Mo, H. J., Mao, S., & White, S. D. M. 1998, MNRAS, 295, 319
Norman, C. A., Sellwood, J. A., & Hasan, H. 1996, ApJ, 462, 114
Peletier, R. F., & Balcells, M. 1996, AJ, 111, 2238
Pfenniger, D., & Norman, C. 1990, ApJ, 363, 391
Raha, N., Sellwood, J. A., James, R. A., & Kahn, F. D. 1991, Nature, 352, 411
Sellwood, J. A., Valluri M. 1997, MNRAS, 287, 124
Sérsic, J. L. 1968, Atlas de Galaxias Australes (Córdoba: Obs. Astron., Univ. Nac. Córdoba)
Shen, J., & Sellwood, J. A. 2004, ApJ, in press (astro-ph/0310194)
Stadel, J. 2001, Ph.D. thesis, Univ. Washington
Terndrup, D. M., Davies, R., L., Frogel, J. A., DePoy, D. L., & Wells, L. A. 1994, ApJ, 432, 518
van den Bosch, F. C. 1998, ApJ, 507, 601
White, S. D. M., & Frenk, C. S. 1991, ApJ, 379, 52